

Fault Identification Algorithm for T-connected Lines based on Traveling Wave Impedance

Xiaoping Gu¹, Jie Yang¹, Jiahao Chen¹ and Hao Wu^{1,*}

¹School of Automation and Information Engineering, Sichuan University of Science & Engineering, Zigong, 643000, China.

Abstract

In order to improve the accuracy of T-connection line fault identification, a new method of T-connection line fault identification based on traveling wave impedance is proposed. The initial voltage and current traveling wave data of each measurement unit at a specific frequency are extracted through S transformation, and the traveling wave impedance of each measurement unit is calculated, and the internal and external faults are distinguished based on the obtained traveling wave impedance value. The simulation results show that the proposed algorithm can identify the internal and external faults of T-connection transmission lines in different fault conditions such as different initial fault angles, different transition resistances, different fault types, and different fault distances.

Keywords

T connection line; S transformation; traveling wave impedance; fault identification.

1. Introduction

The highest probability of failure in the power system is the transmission line. When the transmission line fails, accurate fault diagnosis is of great significance to fault maintenance and fault recovery [1]. Due to the uniqueness of their wiring methods, T-connection lines are becoming more and more widely used in current systems. However, these lines are often accompanied by large power plants and large systems, with high transmission power and heavy load. Once a failure occurs, it may Will cause huge economic losses. Therefore, the study of reliable and effective fault diagnosis methods is of great significance to it [2][6].

At present, domestic and foreign scholars' research on T-connected lines is mainly based on power frequency quantities and transient quantities. Literature [7] uses the ratio of the phasor sum of the three-terminal fault voltage component of the T-connection line to the phasor sum of the fault current component to identify internal and external faults. Literature [8] uses the magnitude of the vector difference between the sum of the three-terminal fault component current of the T-connection line and the maximum current of the three-terminal fault component current and the sum of the currents at the other two ends to establish the criterion to identify the internal and external faults, but the criterion The selection of the braking coefficient will affect the sensitivity and reliability of fault identification. In [9], in order to improve the sensitivity of the criterion for internal faults and the reliability of the criterion for external faults, the criterion proposed in[8] is improved by introducing the maximum current and the maximum current in the three-terminal fault current component of the T-connection line In addition, the sine included angle of the current at both ends is used as the criterion braking coefficient to identify internal and external faults. Literature [10] provides the voltage and current signals measured at the relay terminal of the T-connection line to the second-order Taylor-Kalman-Fourier (T2KF) filter to estimate the instantaneous value of the voltage and current signal phasors. The phasor information is used to obtain the positive sequence

impedance to identify the fault section, but the DC component of the fault current exponentially decays will affect the fault identification. Literature [11] first uses bior3.1 wavelet to decompose the original current signal of the three terminals of the T-connection line, and then reconstructs the decomposed signal, and uses the reconstructed signal to solve the operating current and suppression current of each phase, and finally compares the corresponding phase of the three terminals to run. The relationship between current and suppressed current identifies internal and external faults. Different from the fault recognition algorithm proposed in literature [11], literature [12] compares the polarity of the fault current detected by the Haar wavelet function at each end of the T-connection line to distinguish the internal and external faults, but does not discuss the reliability and safety of the algorithm. And other issues. Reference [13] combined with the high-speed stop filtering properties of the bus, three filters based on mathematical morphology continuously process the current sampling information, and then compare the transients generated by the output faults with three predetermined thresholds respectively to achieve internal and external fault detection Discriminate.

In order to improve the accuracy of T-connection line fault identification, this paper proposes a T-connection line fault identification method based on traveling wave impedance. The initial voltage and current traveling wave data of each measurement unit at a specific frequency are extracted through S transformation, and the traveling wave impedance of each measurement unit is calculated, and the internal and external faults are distinguished based on the obtained traveling wave impedance value. A large number of simulation results show that the proposed algorithm can accurately identify faults inside and outside the T-connection line under various working conditions.

2. Basic Theory of Fault Traveling Wave

Figure 1 shows a 500KV T-connected line. The three branches AO, BO, and CO in Figure 1 are defined as internal branches of the T-connected line, and the remaining branches are external branches.

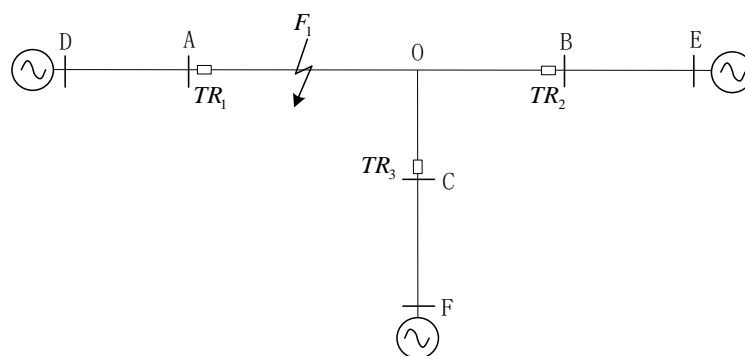


Figure 1. 500kvT connection line

T wiring is composed of branches AO, BO, CO in the area and branches AD, BE, and CF outside the area. Travelling wave protection units TR1~TR3 are installed at the branches near the three ends of A, B and C in the area. When a fault occurs at point F1 on the road AO, the traveling wave starts from the fault point and propagates along the line to both sides, and refraction occurs at the discontinuity of the line wave impedance. For any point on the line from the fault point, the transient state of this point The voltage and current traveling wave are [11]:

$$\begin{cases} \Delta u(x,t) = \Delta u_+(x-tv) + \Delta u_-(x+tv) \\ \Delta i(x,t) = \Delta i_+(x-tv) + \Delta i_-(x+tv) \\ v = 1/\sqrt{LC} \end{cases} \quad (1)$$

In the formula: t is the observation time, L and C are the inductance and capacitance of the unit length line; Δu_+ (Δu_-), Δi_+ (Δi_-) is the forward (reverse) traveling wave of the voltage and current propagating in the positive (reverse) direction of x .

3. Traveling Wave Impedance Calculation based on S Transform

In this paper, Clark phase-mode transformation is used to decouple the phase voltage and phase current, and then the combined modulus method is used to reflect various fault types of T-connection lines [12],

$$\begin{cases} \Delta u_z = 4\Delta u_\alpha + \Delta u_\beta \\ \Delta i_z = 4\Delta i_\alpha + \Delta i_\beta \end{cases} \quad (2)$$

Where: Δu_α and Δu_β are Clark α and β mode voltages respectively; Δi_α and Δi_β are Clark α and β mode currents respectively.

The method used in reference [14] in this paper will perform discrete S transformation on the decoupled fault current and voltage traveling wave modulus, and select the voltage and current sampling points near the initial traveling wave wave head at a single frequency after the fault to calculate the wave impedance clamp.

3.1. S transform

Suppose the discrete time sequence of signal $h(t)$ is $h[kT]$ ($k = 0, 1, 2, \dots, N-1$), where T is the time interval, the discrete Fourier transform of discrete time sequence $h[kT]$ can be obtained as:

$$H\left[\frac{n}{NT}\right] = \frac{1}{N} \sum_{k=0}^{N-1} h[kT] e^{-j\frac{2\pi nk}{N}} \quad (3)$$

In the formula $n = 0, 1, \dots, N-1$.

① When $n \neq 0$, the discrete S of time series $h[kT]$ is transformed into:

$$S\left[kT, \frac{n}{NT}\right] = \sum_{r=0}^{N-1} H\left[\frac{r+n}{NT}\right] e^{-\frac{2\pi^2 r^2}{n^2}} e^{j\frac{2\pi rk}{N}} \quad (4)$$

② When $n = 0$, the discrete transformation of time series $h[kT]$ is a constant, and we can get:

$$S[kT, 0] = \frac{1}{N} \sum_{r=0}^{N-1} h\left(\frac{r}{NT}\right) \quad (5)$$

In the formula $k, n = 0, 1, \dots, N - 1$

After transforming the signal S, a complex matrix reflecting the time-frequency characteristics of the signal is obtained. The behavior frequency information is listed as amplitude and phase information.

3.2. Wave Impedance Calculation

This section takes the initial current and voltage traveling wave measured by measuring unit TR_m to calculate the wave impedance of a specific frequency f_n after S transform as an example. First, S transform the initial voltage and current traveling wave data to obtain the initial voltage and current recovery time Frequency matrix, and then select the 0.1ms time window data after the failure at 60kHz frequency after S transformation to calculate the traveling wave impedance, where $\Delta \dot{U}_{mm}(l)$ and $\Delta \dot{I}_{mm}(l)$ represent the data corresponding to the initial voltage and current at 60kHz after S transformation, where $l = 1, 2, \dots, 20$. Finally, the wave impedance value corresponding to each sampling point is calculated, and the calculation formula is as follows:

$$\dot{Z}_m = \frac{\Delta \dot{U}_m}{\Delta \dot{I}_m} \tag{6}$$

3.3. Fault Identification Process

In this paper, the average value of the wave impedance of 20 sampling points obtained by the measurement of each measurement unit is used for T-connection line fault identification. The fault identification process is shown in Figure 2.

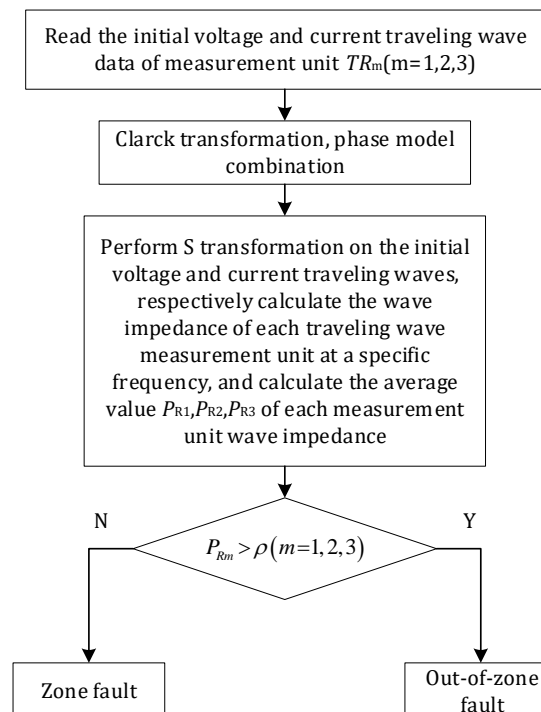


Figure 2. Flow chart of fault identification

Criteria for fault identification:

When $P_{R1} > \rho$ or $P_{R2} > \rho$ or $P_{R3} > \rho$, it is judged as an outside fault, otherwise it is judged as an inside fault, where $\rho = 388$ is.

4. Simulation and Experiment

Use PSCAD/EMTDC electromagnetic transient simulation software to establish the 500kV T-connection line simulation model shown in Figure 1. The line model adopts a frequency-related distributed parameter model that can accurately reflect the transient and harmonic response. The line type uses TOWER: 3H5 tower. The bus stray capacitance is set to $C_m=0.01\mu F$, the simulation sampling frequency is 200kHz, and the length of each branch is AO=300km, BO=200km, CO=150km, AD=170km, BE=150km, CF=180km.

In order to verify the feasibility of the algorithm, simulation experiments were performed on the algorithm from different fault types, different initial fault angles, different transition resistances and different fault distances.

4.1. Simulation Analysis of Different Fault Types

In order to verify the reliability of the algorithm for fault identification under different fault types, this section takes the certification faults of the AO branch in the area and the BE branch outside the area as examples, and simulates 4 groups of different fault types to verify the algorithm. The fault identification results As shown in Table 1.

Table 1. Identification results of different fault types

Inside and outside	Fault type	Fault distance O point/km	Transition resistance/ Ω	Fault initial angle/degree	P_{R1}	P_{R2}	P_{R3}	Recognition result
AO branch (In the district)	AG	135	200	45	356.27	353.63	344.47	In the district
	BCG				347.45	332.30	344.46	In the district
	ABG				356.08	353.70	344.42	In the district
	AC				355.90	353.76	344.36	In the district
BE branch (outside the area)	BG	270	300	100	350.64	388.21	351.70	Outside
	ABG				350.68	388.21	351.67	Outside
	ACG				350.68	388.21	351.67	Outside
	BC				350.69	388.21	351.66	Outside

It can be seen from the above table that the proposed algorithm can accurately identify the internal and external faults of the T-connection transmission line under different fault types.

4.2. Simulation Analysis of Different Initial Fault Angles

In order to verify the reliability of the algorithm for fault identification under different fault initial angles, this section takes the certification faults of the AO branch in the area and the CF branch outside the area as examples, and simulates 4 groups of different fault initial angle faults to verify the algorithm. The recognition results are shown in Table 2.

Table 2. Recognition results of different fault initial angles

Inside and outside	Fault initial angle/degree	Fault distance O point/km	Transition resistance/ Ω	Fault type	P_{R1}	P_{R2}	P_{R3}	Recognition result
AO branch (In the district)	5	100	300	CG	355.47	356.63	343.18	In the district
	45				340.20	346.37	356.46	In the district
	60				341.79	350.50	351.17	In the district
	90				340.28	344.04	357.60	In the district
CF branch (outside the area)	45	230	100	BCG	350.93	351.32	388.20	Outside
	60				350.43	350.66	388.20	Outside
	90				350.07	351.23	388.19	Outside
	100				351.14	351.67	388.21	Outside

It can be seen from the above table that the proposed algorithm can accurately identify the internal and external faults of the T-connected transmission line when the initial fault angle is different.

4.3. Simulation Analysis of Different Transition Resistance

In order to verify the reliability of the algorithm for fault identification under different fault transition resistances, this section takes the certification failure of the BO branch in the area and the AD branch outside the area as examples, and simulates 4 groups of different transition resistance faults to verify the algorithm. The results are shown in Table 3.

Table 3. Different fault transition resistance identification results

Inside and outside	Transition resistance/ Ω	Fault distance O point/km	Fault initial angle/degree	Fault type	P_{R1}	P_{R2}	P_{R3}	Recognition result
BO branch (In the district)	100	135	25	AC	346.87	364.19	351.97	In the district
	200				346.87	364.19	351.97	In the district
	300				346.87	364.19	351.97	In the district
	400				346.87	364.19	351.97	In the district
AD branch (outside the area)	100	405	45	ABG	388.21	350.39	351.12	Outside
	300				388.21	350.39	351.12	Outside
	300				388.21	350.39	351.12	Outside
	400				388.21	350.39	351.12	Outside

It can be seen from the above table that the proposed algorithm can accurately identify the internal and external faults of the T-connection transmission line when the transition resistance of different faults fails.

4.4. Simulation Analysis of Different Fault Distances

In order to verify the reliability of the algorithm for fault identification under different fault distance resistances, this section takes the certification faults of the CO branch in the area and the BE branch outside the area as examples, and simulates 4 sets of different transition distance barriers to verify the algorithm. Fault identification The results are shown in Table 4.

Table 4. Different fault distance identification results

Inside and outside	Fault distance O point/km	Transition resistance/ Ω	Fault initial angle/degree	Fault type	P_{R1}	P_{R2}	P_{R3}	Recognition result
CO branch (In the district)	110	200	60	ACG	351.74	356.50	344.61	In the district
	80				349.83	354.87	340.26	In the district
	60				346.76	341.83	339.54	In the district
	20				344.46	346.49	335.84	In the district
BE branch (outside the area)	325	100	90	ACG	351.21	388.19	350.04	Outside
	295				351.08	388.19	349.57	Outside
	260				350.24	388.22	351.08	Outside
	215				350.18	388.22	351.71	Outside

It can be seen from the above table that the proposed algorithm can accurately identify the internal and external faults of the T-connection transmission line when the fault is at different fault distances.

5. Conclusion

This paper proposes a T-connected line fault identification algorithm based on traveling wave impedance. After a lot of simulation analysis, the proposed algorithm can be accurate under different fault types, different transition resistances, different fault initial angles, and different fault distances. Identify faults inside and outside the T-connection line.

Acknowledgements

Sichuan University of Science and Engineering Postgraduate Innovation Fund Project (y2019011).

References

- [1] He Zhengyou. Application of wavelet analysis in power system transient signal processing[J]. Beijing: China Electric Power Press., 2011. (In Chinese)
- [2] Mahamedi Behnam, Sanaye-Pasand Majid, Azizi Sadegh. Unsynchronised fault-location technique for three-terminal lines[J]. IET Generation Transmission & Distribution, 2015, 9(15): 2099-2107.
- [3] An Jianfeng. Application of T-connection line differential protection [J]. Power System Protection and Control, 2008(21): 93-96. (In Chinese)
- [4] Shu Hongchun, Gao Feng, Chen Xueyun, et al. Research on fault location algorithm of T-type transmission system[J]. Proceedings of the Chinese Society of Electrical Engineering, 1998(06): 41-45. (In Chinese)
- [5] Zhang Wujun, Wang Huifang, He Benteng. Traveling wave differential protection for T-connection lines [J]. Automation of Electric Power Systems, 2007(03): 61-66. (In Chinese)
- [6] Liao Zeyou, Bao Weilian, Yang Weina, et al. Current status and prospects of high-voltage line current differential protection[J]. Relay, 1999(01): 6-9+23. (In Chinese)
- [7] Suonan Jiale, Deng Xuyang, Li Ruisheng, et al. New principle of T-connection line pilot protection based on the integrated impedance of the fault component[J]. Electric Power Automation Equipment, 2009, 29(12): 4-9. (In Chinese)
- [8] Gao Houlei, Jiang Shifang. Research on the new criterion of T-connection line current longitudinal differential protection[J]. Relay, 2001(09): 6-9+16. (In Chinese)
- [9] Liu Jing, Tai Nengling, Li Shen. Research on T-type line current differential protection [J]. Electric Power Automation Equipment, 2008(10): 58-63. (In Chinese)
- [10] Kumar Abhishek; Babu P. Suresh, Babu NV Phanendra. Taylor-Kalman-fourier filter based back-up protection for teed-transmission line[C]. International Conference on Computing, Communication and Networking Technologies (ICCCNT). JUL 03 -05, 2017.
- [11] Bhalja B, Maheshwari R. P. New differential protection scheme for tapped transmission line[J]. IET Generation Transmission & Distribution, 2008, 2(2): 271-279.
- [12] Eissa M.M. A new digital relaying scheme for EHV three terminal transmission lines[J], Electric Power Systems Research. 2005, 73(2): 107-112.
- [13] Khodadadi M, Shahrtash S.M. A New Noncommunication-Based Protection Scheme for Three-Terminal Transmission Lines Employing Mathematical Morphology-Based Filters[J]. IEEE Transactions on Power Delivery, 2013, 28(1): 347-356.
- [14] Bai Jia, Xu Yuqin, Wang Zengping, et al. Traveling wave current polarity comparison directional protection principle based on combined modulus[J]. Power System Technology, 2005(13): 69-72. (In Chinese)